THE PENNSYLVANIA STATE UNIVERSITY
SCHREYER HONORS COLLEGE

DEPARTMENT OF BIOLOGY

CONSERVATION OF ETHER-A-GO-GO FAMILY POTASSIUM CHANNELS IN CNIDARIANS

ALEXANDRA MARTINSON
SPRING 2013

A thesis
submitted in partial fulfillment
of the requirements
for a baccalaureate degree
in Biology
with honors in Biology

Reviewed and approved* by the following:

Timothy Jegla
Assistant Professor of Biology
Thesis Supervisor

Stephen W. Schaeffer
Professor of Biology
Honors Adviser

* Signatures are on file in the Schreyer Honors College.

ABSTRACT

The Ether-a-go-go family of potassium channels consists of three functionally independent gene families, *Eag* (Kv10), *Erg* (Kv11) and *Elk* (Kv12), conserved between insects and mammals. All three gene families encode sub-threshold voltage-gated potassium channels with distinct biophysical properties. Ether-a-go-go family channels differ from other potassium channels by the presence of a distinct complement of cytoplasmic modulatory domains (EAG, PAS, cNBD) that regulate channel function. We characterized the Ether-a-go-go family in a cnidarian, *Nematostella vectensis* (starlet sea anemone), to determine which properties of these channels have been conserved throughout the history of the nervous system. Cnidarians diverged from the vertebrate line early in metazoan evolution and the first nervous system evolved in a late common ancestor of vertebrates and Cnidarians. We find that all three gene families (*Eag*, *Erg* and *Elk*) are present and highly conserved in *Nematostella*. The *Nematostella Eag* and *Elk* families are represented by a single gene (*NvEag1* and *NvElk1*), whereas the *Nematostella Erg* family has been expanded to five genes (*NvErg1-5*). *NvErg2-5* interestingly lack the characteristic EAG and PAS domains at the N-terminus. We examined functional conservation by comparing the properties of *NvEag1* and *NvErg1* currents to currents produced by their mammalian orthologs *Mouse Eag2* and *Mouse Erg3*. We find that the distinctive gating characteristics of *Eag* and *Erg* genes are conserved between mammals and Cnidarians. Like mammalian Ether-a-go-go family channels, the *Nematostella* channels are highly sensitive to changes in external pH. Their

pH sensitivity is influenced by Ether-a-go-go family-specific acidic charges in the voltage sensor.

TABLE OF CONTENTS

LIST OF FIGURES

LIST OF TABLES

ACKNOWLEDGEMENTS

Thank you to Dr. Tim Jegla first and foremost. After introducing the idea of an evolutionary project you let me own the entirety of the project, taking the time to teach me the more difficult techniques, such as electrophysiology. Without your mentorship this project could never have come to fruition. I look forward to continuing to work with you after the due date to publish these and other results that we will inevitable uncover before my time here at Penn State ends.

I would also like to thank Dr. Mark Martindale for generously providing us with not only the starting breeder *Nematostella* so that we could start our own line, but also for the starting cDNA material, without which my thesis project could not have started as quickly.

My wonderful lab-mates have also supported me throughout this thesis project. Alham Sadaat trained me in all of the molecular cloning techniques before this project started and has always served as a great resource. Colin Ackerman generously provided cDNA that he had made from *Mouse*. Hansi Liu and Xioufan Li were always in the lab when I had questions about the electrophysiology rig or had trouble with my RNA injections. All of you truly helped me with this project, thank you so much.

Chapter 1: Introduction

Potassium channels

Potassium channels have a variety of funct1ions that are vital to life. These channels contribute to negative resting potential by opening to let out positive ions and hyperpolarize the cell. Additionally, potassium channels are known for controlling excitability and specifically dampening excitation, which requires a net influx of positive charge. Therefore, potassium channels have the ability to make it more difficult to fire an action potential. The other major function of potassium channels *in vivo* is to repolarize the cell after an action potential to return to and maintain resting potential. Collectively, these roles give potassium channels the ability to determine the shape and frequency of action potentials. Potassium channels can shape an action potential such that it is short and sharp, or sustain it longer by adjusting the rate and length of channel opening (Hille 131-167).

Due to these important and diverse functions, there are many functionally distinct potassium channels present in higher animals. The human genome contains 78 genes that encode pore-forming subunits of potassium channels; these channels are gated by many stimuli such as voltage activation and ligands such as calcium and g-proteins (Jegla et al., 2009). The functional diversity of potassium channels allows them to participate in most physiological processes, and they are a rich target class for therapeutic intervention (Jegla et al., 2009). For instance, one voltage gated potassium channel, Kv1.3, found in humans has been identified as a target for drug development due to its ability to regulate Ca^{2+} intake and its involvement in the signaling

pathways responsible for the proliferation of cells such as T-lymphocytes and prostate cancer cells (Wickenden, 2002).

EAG Family Channels

We are currently studying the Ether-a-go-go (EAG) family of voltage-gated potassium channels. This family of channels includes three distinct subfamilies – *Eag*, *Erg* and *Elk*. Two of these subfamilies, *Eag* and *Erg* will be functionally characterized in the sea anemone *Nematostella vectensis* in this thesis. Although each subfamily has individual characteristics, the entire EAG family functions *in vivo* to control excitability (Jegla et al., 2009). EAG channels are highly expressed in the nervous system and therefore, they have the ability to modulate communication and activity of neurons. *Elk* channels activate at very hyperpolarized voltages and are pertinent regulators of sub-threshold current (Jegla, 2009). Zhang et. al. (2010) showed that a human *Elk* channel controls excitability of forebrain pyramidal neurons and that a loss of the channel leads to epilepsy. The *Elk* channel (Kv12.2) knock-out mice were seen to have intermittent seizures and significantly reduced tolerance for chemoconvulsants (Zhang et al., 2010). EAG family channels are involved in other processes in the brain such as an Erg channel that is implicated in regulating the mouse auditory brainstem excitability (Hardman and Forsythe, 2009). In humans, the *hERG1* channel has been proven crucial to cardiac action potentials, and mutations lead to long QT syndrome and potentially life-threatening arrhythmias (reviewed in Sanguinetti and Tristani-Firouzi, 2006). These and many other disease implications create an impetus to discern the function of EAG family channels in *Nematostella* to determine if their role in the nervous system might be physiologically conserved.

EAG family channels are characteristically activated by sub-threshold voltages which confers upon them a unique role *in vivo*. Threshold as used in this thesis is defined as the voltage required for a neuron to fire an action potential. When EAG family channels are expressed in a neuron, they create an outward K^+ current which the neuron must overcome to reach threshold and fire an action potential. This influence can be explained by the equation V = I*R. The open EAG family channels will lower membrane resistance meaning that increased input is necessary to achieve a given voltage change (Jegla et al., 2009).

Many of the EAG family channel specific properties originate from the structure of the channels which can be seen in Figure 1. All EAG family channel subunits share the same general structure. Each contains six transmembrane (TM) domains; TM1-4 create the voltage sensor while TM5, TM6 and the selectivity filter form the pore through which K^+ flows. Four of these subunits come together to form one tetrameric channel. Figure 1 shows two views; on the left is a top view of the tetrameric structure while the right shows a view from the side which demonstrates how the domains exist in the plasma membrane by depicting two subunits. EAG family channels typically contain a cytoplasmic PAS domain at the N-terminus and a cNBD domain near the C-terminus that modulate channel function (Jegla et al., 2009).

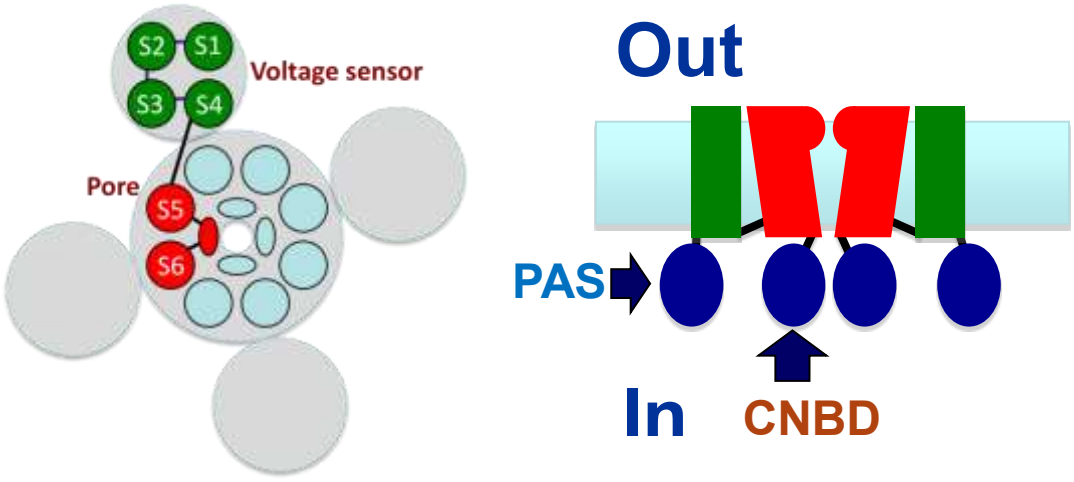

Figure 1. Structure of a typical EAG Family Channel

Within the voltage sensor are conserved residues that have been shown to contribute to external pH sensitivity of EAG channels (Kazmierczak et al., submitted). *Eag*1, *Erg*1 and *Elk*1 had previously been shown to be inhibited by increasing acidity (Terlau et al., 1996 Anumonwo et al., 1999; Berube et al., 1999; Jo et al., 1999; Terai et al., 2000 Shi et al., 1998). With decreasing external pH (increased concentration of protons) it was found that the EAG family channels open at relatively depolarized values. Due to less sub-threshold opening, lower external pH can thus lead to more excitability (Kazmierczak et al., submitted). Two EAG-specific acidic residues in the TM2 and TM3 domains were found to be important for pH sensitivity and when altered reduced pH sensitivity greatly in the channels (Kazmierczak et al., submitted). We studied the role of these residues in pH sensitivity in the EAG family channels cloned from *Nematostella*.

Cnidarians as a model system

We studied the functional evolution of EAG family channels to determine if the properties of channels have been evolutionarily conserved and thus, which properties are most physiologically relevant. To study EAG-family channels utilizing a functional evolution technique, we needed a practical model system that was ancient compared to Bilaterians. Cnidarians are the ideal phylum for evolutionary study because they diverged before the radiation of Bilaterians, but possess nervous systems and many of the neuronal signaling molecules that are conserved in Bilatarians. This branch point is also near the origin of the central nervous system, therefore properties of channels conserved between mammals and Cnidarians are likely fundamentally important to the channel's physiological role. (Putnam et al., 2007, Jegla et al., 2009)

The Cnidarian *Nematostella vectensis* was chosen for our study for several reasons. The genome of *Nematostella* has been published and annotated, which allowed for easy identification of channel genes for cloning and subsequent functional expression of EAG family channels (Putnam et al., 2007). Additionally, another family of K^+ channels was recently successfully characterized using a functional evolution technique with *Nematostella* (Jegla et al., 2012). The increasing popularity of *Nematostella* as an evolutionary model system also allows for many future research possibilities. For example, transgenic lines of *Nematostella* were recently created and could be used for behavioral experiments to further discern the role of EAG family channels *in vivo* (Renfer et al., 2010).

The traditional view was that Cnidarians had a simple, decentralized nerve net, but upon analysis of the *Nematostella* genome, scientists found surprising complexity. It was found that the structure of the genome is very similar to that of eumetazoans. The *Nematostella* genome, like that of modern day vertebrates, is intron rich, has a similar number of exons per gene, and a similar number of genes (Putnam et al., 2007). This complexity extends to the ion channels contained in the *Nematostella* genome as well; *Nematostella* possess 43 out of 46 ion channel families that have been conserved throughout the history of Bilaterians. This number of ion channels suggests unexpected functional complexity of the nervous system in *Nematostella*, which, though not centralized, contains distinct classes of neurons and cnidocytes (stinging cells) (Marlow et al., 2009).

Another surprising result has shown that the phyla Ctenophora may be more ancient than previously thought. Schnitzler et al (2013) sequenced the first Ctenophore genome and the results suggested that Ctenophores may have split from the main metazoan lineage before the divergence of Cnidarians and Bilaterians. However, Ctenaphora genome sequence was not available at the time this thesis project began. Additionally, Ctenaphores do not appear to have EAG-family channels, which solidified our decision to use the Cnidarian *Nematostella*.

Experimental Aims and Hypothesis

EAG family channels have been shown to regulate neuronal excitability in higher animals and have been conserved since before the phyla Bilateria and Cnidaria diverged. The aim of this study is to functionally compare the Cnidarian (*Nematostella*) and Bilatarian channels to discover which properties (and thus physiological roles) have been conserved. We identified and cloned the EAG family channel genes from *Nematostella* and functionally expressed them to compare gating kinetics, sub-threshold activation and pH sensitivity. Our hypothesis was that the characteristic sub-threshold activation of the EAG family channels would be conserved due to its important physiological function *in vivo* in higher animals. However, we were unsure about the degree of similarity between pH sensitivity and specific gating kinetics of the channels in *Nematostella* and mammals as their role *in vivo* and importance has not previously been clearly defined for all EAG family channels.

Chapter 2

Materials and Methods

Identification of Genes

To identify *Nematostella* EAG family genes, we searched for homologs of *Mouse* EAG family genes in the draft genome of *Nematostella* curated by the Joint Genome Institute (JGI) (http://genome.jgipsf.org/pages/blast.jsf?db=Nemve1). We used TBLASTN to search for *Nematostella* genome sequences similar to the *Mouse* EAG family protein sequences (Altschul et al., 1997). Especially across species that are significantly different such as *Mouse* and *Nematostella*, amino acid sequences will be more conserved than nucleotide sequences because selection acts to maintain protein function rather than the third position of codons. The individual nucleotide sequence of an organism may vary in unpredictable ways simply due to a genome bias for a certain nucleotide. After the initial TBLASTN search to identify gene loci, we used a combination of homology-based prediction, verified expressed sequence tags (ESTs), and existing exon predictions to assemble putative coding sequences and amino acid sequences (Altschul et al., 1997). The predicted amino acid sequences were then compared to *Mouse* REFSEQ by BLASTP to identify the top hits (Altschul et al., 2007). Genes found in the initial searches of the *Nematostella* genome that had reciprocal best hits with *Mouse* EAG channels were considered to be EAG family channels. This step was necessary because searches also identified cyclic nucleotide gated (CNG) ion channels and other voltage-gated potassium channels, and served as a check that we had identified the true EAG family channels.

Molecular Cloning

The templates used for all cloning were cDNAs made from *Nematostella* and *Mouse.* The *Nematostella* cDNA library used for the first round of cloning was generously provided by Mark Martindale (Kewalo Marine Laboratory, University of Hawaii) and was comprised of mixed life stages of *Nematostella*. All subsequent *Nematostella* cDNA was made from RNA we harvested ourselves using the QIAGEN RNeasy kit and 35mg of starting material (adult *Nematostella*). The isolated RNA was then reverse transcribed to create cDNA using the Invitrogen Reverse Transcription kit with Superscript III enzyme. *Mouse* cDNA was provided by lab mate Colin Ackerman.

Primers were designed to clone the full coding region of each *Nematostella* EAG family channel. Most coding regions could be confidently predicted based on similarity to mammalian EAG family channels and verified EST sequences, but the 3' ends of *NvErg1* and *NvEag1* had to be experimentally determined. We made a series of antisense primers in potential 3' exons for each gene and paired them with sense primers upstream of an intron/exon boundary and for each gene obtained one product with the true 3' end. Full length products were assembled using overlap PCR, and cloned into an expression vector, POX-ER. At least 3 clones were fully sequenced to generate a consensus sequence of the gene. Only clones that matched the consensus sequence were used for expression. *NvEag1E478D* and *NvErg1G308D* mutants were made using PCR based mutagenesis and sequence verified.

Sequence Alignment and Phylogenetic Tree Reconstruction

EAG channel sequences from *Nematostella* (sea anemone), *Mus musculus* (mouse), *Xenopus* (frog), *Fugu* (pufferfish), *Rattus* (rat), *Homo sapiens* (human), *Gallus* (chicken),

Capitella teleta (polychaete worm), *Anopheles gambiae* (mosquito), *Drosophila melanogaster* (fruit fly), *Strongylocentrotus purpuratus* (sea urchin), *Daphnia pulex* (water flea), *Caenorhabditis elegans* (nematode), and *Caenorhabditis briggsae* (nematode), were aligned using ClustalW protocol as implemented in the program Mega 5 (Tamura et al., 2011). The sequence alignment was used to create a Bayesian Tree with the MrBayes program (Ronquist et al., 2011). The resulting tree contains the most likely evolutionary relationship and also includes on each branch the posterior probability corresponding to that branch point. The Bayesian inference tree is created such that the program optimizes tree topology after a large number of generations and estimates the posterior probability for each branch point. The tree included in this thesis was created using MrBayes to run two independent trials of four chains for greater than one million generations under a mixed model. The first 25% of the trees were discarded and the resulting phylogeny displayed is based on the consensus of the remaining trees from the two runs. The posterior probability values correspond to the frequency with which the consensus tree branch point is found in individual trees.

Electrophysiology

The finished clones (*NvErg1*, *NvEag1*, *MmErg3*, *NvEag1E478D*, and *NvErgG308D*) were digested with Not1from NEB (Ipswich, MA) to linearize the DNA. The linearized DNA was then used to make capped run-off cRNA transcripts using the T3 mMessage mMachine kit from Life Technologies. Samples were precipitated in LiCl and purified with ethanol prior to suspension in nuclease free water supplemented with SUPERase-In from Life Technologies, an RNase inhibitor.

We expressed the constructs in *Xenopus* oocytes which were purchased from Nasco and de-folliculated using Type II collagenase (1 mg/ml). A 50 nl volume of the RNA (1-50ng)

described above was injected into the oocytes. After injection, the oocytes were incubated one or two days at 18 degrees Celsius in a culture solution made of (96 mM NaCl, 2 mM KCl, 2 mM CaCl2, 1 mM MgCl2, 5 mM HEPES, pH 7.2) supplemented with 2.5 mM Na-pyruvate, 100 U/mL penicillin and 100 μg/mL streptomycin. Following incubation, electrical recordings were made using standard two electrode voltage clamp technique in which the voltage is manipulated by the experimenter to determine the amount of ion current passing through the channel. Through this technique, time course and probability of channel activation can be determined at a variety of voltages to characterize voltage dependence. The specific protocols used to gather data from each channel will be described in the context of the results as the protocols were dependent upon the channel and property being studied.

The electrodes used for the recordings were filled with 3 M KCl and had a low resistance between 0.5 and 1 MΩ to obtain fast voltage clamp. Recordings were performed in a variety of solutions that were adjusted to pH 8,7, and 6 using methanesulfonate major anion instead of Cl^- to limit contamination with native oocyte chloride currents. The base solution was comprised of 98 mM NaOH, 2 mM NaCl, 2 mM KCl, and 5 mM HEPES. The solution covered the egg and constant perfusion flowed over the egg during the recording to reduce potassium accumulation during channel activation. Additionally, unless otherwise noted chemical reagents were all purchased from Sigma-Aldrich (St. Louis, MO).

The results were analyzed using the pCLAMP (Molecular Devices, Sunnyvale, CA) program to output data points. Then, the Origin8.1 program (Origin Lab, Northampton, MA) was used for the graphing, fitting and other data analysis of the raw electrophysiological data. All electrophysiological data was fitted using a single Boltzmann distribution, $f(V) = (A_1 + A_2)/(1 + e^{(V-V_{50}/s)}) + A_2$, where A_1 and A_2 are asymptotes, V_{50} is the half-maximal point and s is the slope

factor. Some of this data analysis and the 2 tailed student *t*-test were performed in Microsoft Excel (Microsoft, 2010).

Chapter 3

Results and Discussion

All of the EAG family genes were found to exist in the *Nematostella* genome, and *NvErg1*, *NvEag1*, *NvElk1* and *NvErg4* were all cloned, although *NvElk1* was partially cloned and *NvErg4* was not functionally expressed at the completion of this thesis. To definitively show the relationship between the *Nematostella* EAG channels and those of higher animals, we created a Bayesian inference tree seen in Figure 2. In Figure 2, *Nematostella* sequences are highlighted in red, and red asterisks indicate the channels that were cloned for this study. Of those, *NvErg1*, *NvEag1* and *mERG3* were functionally characterized in this study and *mEAG2* was characterized previously in lab. Vertebrate sequence branches are blue and placozoan branches are green. Placozoans are the most primitive known eumetazoans and do not have a nervous system, therefore in this tree they serve as an outgroup (Srivastava et al., 2008). The *Eag*, *Erg* and *Elk* subfamilies are indicated at the right margin. Posterior probabilities less than one are shown while those equal to one are omitted as they mean the branch point showed the same relationship in all trees created. From the posterior probabilities throughout the figure, one can deduce that this tree is very likely to represent the true evolutionary relationship between the EAG Family channels in a variety of organisms.

Figure 2 highlights the fact that all three subfamilies under the EAG family channels are present in *Nematostella* and each have at least one clear ortholog of the EAG subfamily gene found in higher animals. The orthologous EAG family genes all stem from a single common ancestor gene, and there are 18 distinct vertebrate orthologs in the *Elk* and *Erg* subfamilies, and 12 orthologs in the *Eag* subfamily. The EAG family homologs branch before radiation of Bilaterian sequences which is consistent with the evolutionary relationship of the organisms. Interestingly, the *Erg* subfamily has a *Nematostella*-specific expansion, *NvErg2-5*, that the tree suggests occurred after separation of Cnidarians and Bilaterians. *NvErg2-5* are closely grouped in the genome suggesting a recent gene duplication event. The function of the additional channels found in *Nematostella* is unknown and their function is a future research target of ours.

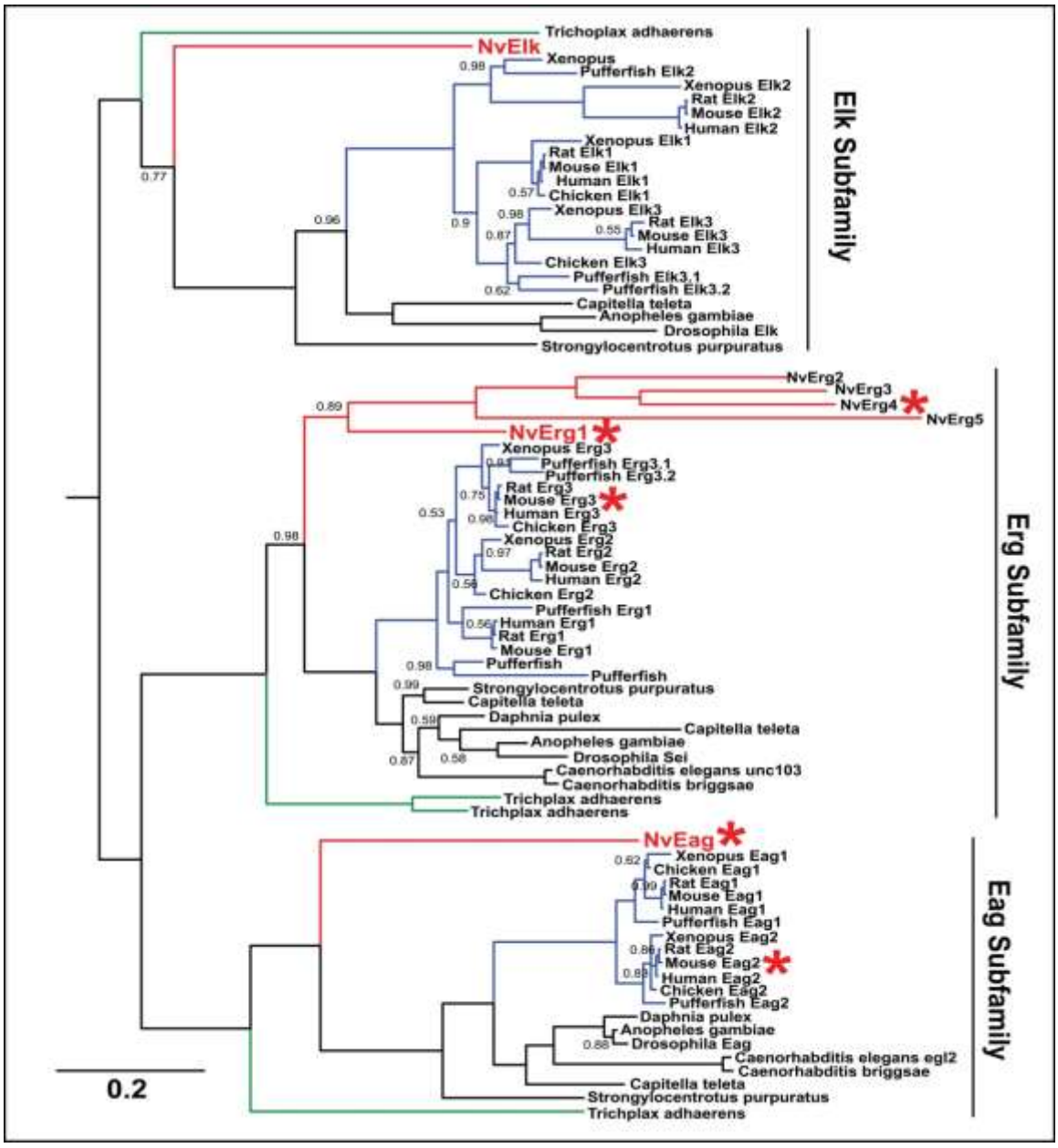

Figure 2. Bayesian inference phylogeny of the metazoan Ether-a-go-go-family

After cloning *NvEag1*, we used the sequence obtained to create an alignment that includes sequences of Bilaterian homologs, specifically Mouse and Drosophila Eag subfamily channel sequences which can be seen in Figure 3. The functional domains are underlined and labeled for ease of identification. The universally conserved residues are highlighted in black, and one can see they are concentrated around functional domains; linker regions are generally not

conserved. Figure 3 was the first piece of evidence to reinforce that the Eag subfamily homolog in *Nematostella* is similar to that found in bilaterially symmetric animals, and in fact has many of the same residues. Based on this alignment we predicted that the channels would behave similarly.

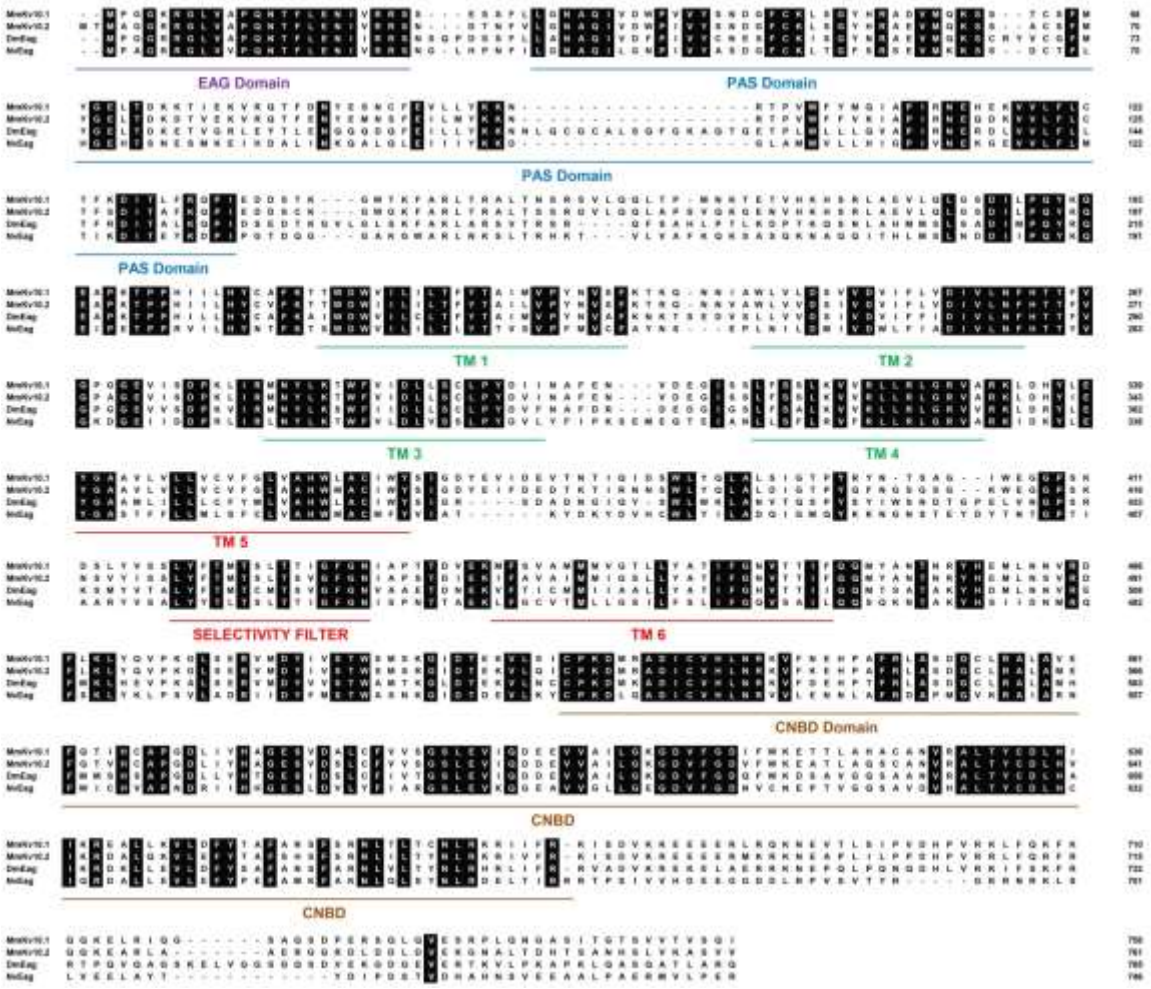

Figure 3 *Eag* Channel Alignments of cloned *Nematostella, Drosophila* and *Mouse*

Figure 4 shows the same alignment for the *Erg* subfamily channels, including the amino acid sequence obtained from cloning *Nematostella Erg1* and from Mouse and Drosophila sequences. This figure is similar to Figure 3, and is even more extreme in conservation of domain specific residues. One can see all conservation is located within the domains and there is virtually no conservation in the linker regions and C-terminus. The N-terminus similarities

between Mouse and *Nematostella NvErg1* channels are highlighted in red as the *DmErg* channel appears to lack the PAS domain. We also hypothesized the function of *NvErg1* might be similar to vertebrate orthologs based on this sequence alignment. Interestingly, *NvErg2-5* also appear to lack the N-terminal domains, but are still most closely related to *NvErg1*.

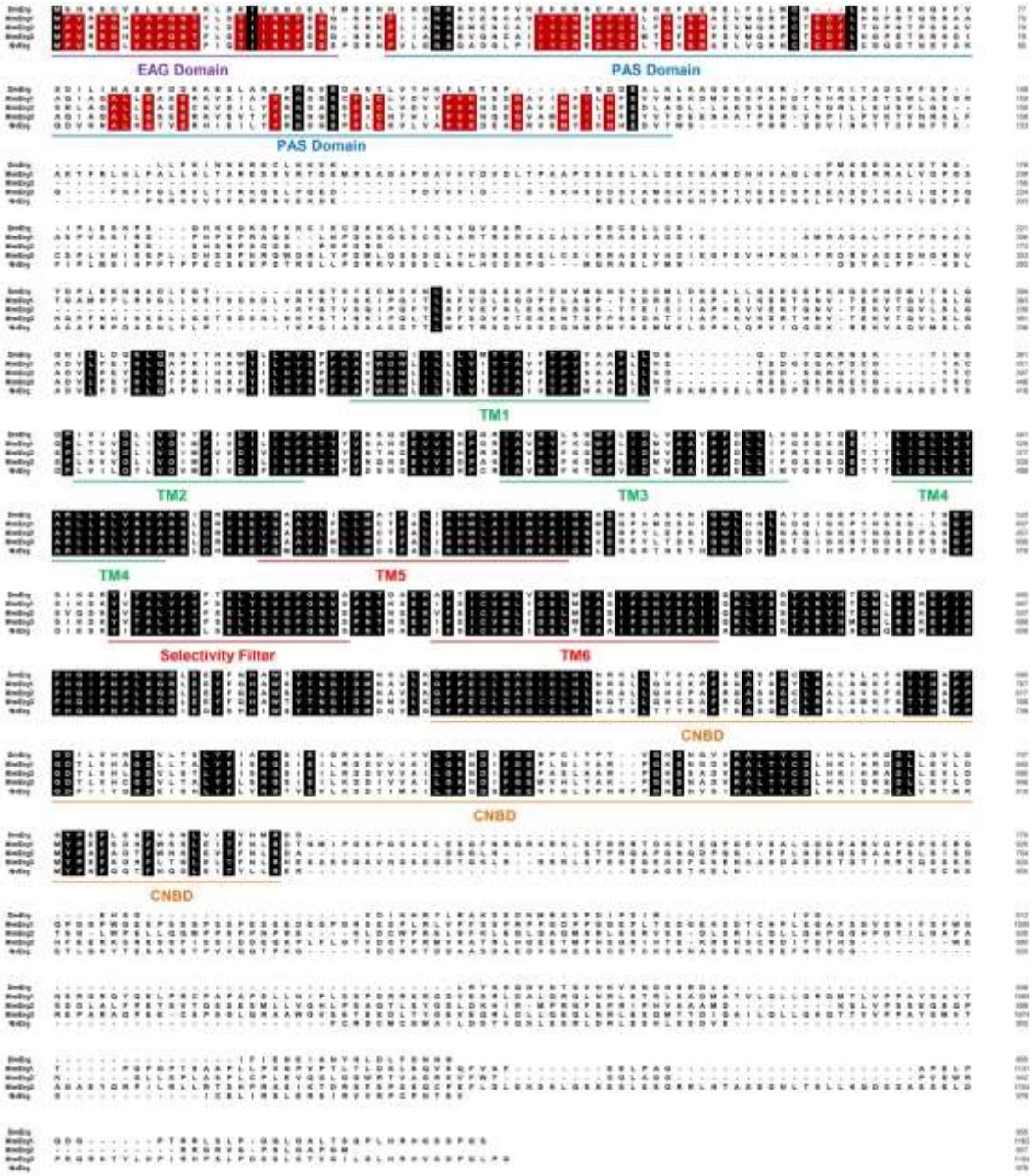

Figure 4. *Erg* Channel Alignments of cloned *Nematostella*, *Drosophila* and *Mouse*

After cloning, the constructs were functionally expressed to definitively characterize *NvErg1* and *NvEag1* and determine which, if any, features found in the higher metazoan homolog channels were similar in *Nematostella*. Figure 5 shows the functional expression of *NvErg1* and *MmErg3*.

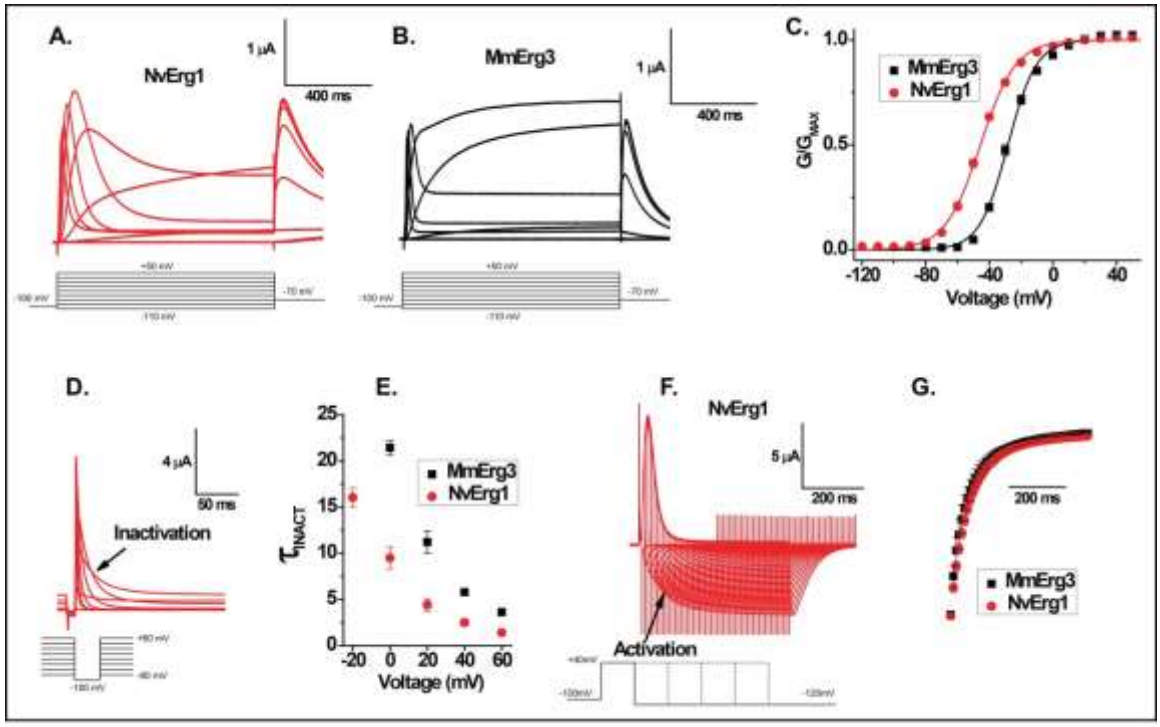

Figure 5. Functional Expression of *NvErg1* and *MmErg3*

Panel A in this figure shows an example trace taken from a recording of the *NvErg1* channel. The currents were recorded in response to voltage steps ranging from -110 to + 50mV in 20 mV increments. These steps capture the current flowing through the ion channel at a large range of voltages and the current shape is shown in Panel A. E_K^+, the equilibrium potential of potassium, which is dependent on electrical driving force as well as concentration gradient, is around -90mV in our recordings mostly due to the extremely large concentration of potassium within the egg and the low potassium external solution. Since the *NvErg1* channel activates above -90 mV, the only current seen in Panel A is outward current, and the same is true for the example trace recorded from *MmErg3* in Panel B. The *MmErg3* example trace seen in Panel B

has many similarities with the example trace seen from *NvErg1* in Panel A. These channels are activated by depolarization but subsequently inactivate during strong depolarizations. Therefore, the amount of current passing through the channels decreases after the initial peak in the trace. The amount of current temporarily increases during the tail current, as a large number of inactivated channels synchronously recover to the open state before slowly closing.

The fast inactivation of *Erg* channels is intrinsic to the function of *hERG1* in humans which mediates cardiac plateau action potentials (Grunnet et al., 2008). The rapid inactivation of this channel and relatively slow activation allows the channel to turn on slowly during the plateau phase of the cardiac action potential (Grunnet et al., 2008). Interestingly, the *NvErg1* channel shows a peak in current after the repolarization to -70mV for the tail currents. This is very similar to the peak in current seen in the repolarization phase of the cardiac plateau action potential (Grunnet et al., 2008). Therefore, the characteristics of the *hERG1* channel that contribute to action potential shape are also present here in the *NvErg1* channel and have thus been evolutionarily conserved, and may indicate the presence of plateau action potentials in *Nematostella*.

Panel C shows the G/V curves, which represent the voltage dependence of activation, for both the *NvErg1* channel and the *MmErg3* channel. From traces such as those shown in Panel A and B, isochronal tail currents were taken at -70mV to create the G/V curves. The tail current measurements from traces led to data points, which are the mean ± S.E. of n= 9-15, each recorded at -70mV. During voltage steps, the current size varies with both the open probability and the electrochemical driving force. The reason we take isochronal tails when voltage is constant is that only open probability varies. This allows simple determination of open probability because it is directly proportional to current size. The G/V curve is a single Boltzmann Distribution fit used to estimate midpoint and slope of the relationship between the data points. The x-axis of the G/V curve represents the voltage and the y-axis shows the fraction of channels open at a given voltage

denoted by the value G/G_{max} where G stands for conductance at the given voltage and G_{max} stands for maximal conductance. Therefore, the amount of current passing through the channel was measured during the tail recordings and divided by the maximum tail current observed to determine number of channels open. G/V curves demonstrate the voltage-activation range of the channels and allow calculation of the voltage at which half of the channels are open, otherwise denoted as V_{50}, which is often used to compare channels.

From the G/V curve shown in Panel C, taken from recordings at pH 7, one can observe that the voltage dependence is similar for both channels. One can also see that the *NvErg1* channel curve is slightly hyperpolarized in comparison to that of the *MmErg3* channel, which is also reflected in the V_{50} values of the two channels. The V_{50} value for the *NvErg1* channel at pH 7 is -45.6 ± 0.8 mV and the V_{50} for MmErg3 is -28.3 ± 1 mV, however the *NvErg1* channel starts to open in earnest around -75mV and the *MmErg3* channel starts to open around -50mV as can be seen in the G/V curve. As the action potential threshold varies in cells from around -55mV to -30mV, these channels both have substantial open probability in the sub-threshold range. This corroborates the conserved role of *Erg* subfamily channels in modulation of sub-threshold excitability.

The rate of inactivation for *NvErg1* is shown in Panel D of Figure 5. The data points from recordings of *NvErg1* have both activation and inactivation occurring simultaneously, making it impossible to discern the difference between the two without a specific protocol to separate them. The protocol to record inactivation rate of *NvErg1* consisted of steps from -80mV to +60mV followed by a brief repolarization by a -100mV pulse and then a step back up to the original voltage from -80mV to +60mV. The initial depolarization opens all of the channels normally opened at that voltage, but then some of them will start to inactivate. The subsequent repolarization to -100mV allows the channels to recover from inactivation if they have already started to inactivate, however, is short enough that they do not deactivate. Then, during the

second depolarization all of the channels are already open and the inactivation proceeds without contamination from activation and channels that rapidly inactivate are captured by the measurement. Panel D shows that the inactivation of the *NvErg1* is rapid, note that the timescale is very fast and distinct in this panel compared to others.

From the data collected about the inactivation of the channels, the time constant of inactivation, τ, is plotted vs. voltage in Panel E of Figure 5. τ is derived from a single exponential fit to the inactivation curve when the value reaches 1/e decay which is proportional to the time it takes the channel to inactivate, and voltage is shown on the x-axis. Again, this graph shows the similarities between the *NvErg1* channel and *MmErg3* channel. One can see that it takes the channels longer to inactivate at lower voltages and at higher voltages they inactivate more quickly which reinforces the idea that these channels are active at sub-threshold currents – there is little inactivation there and virtually a steady state current produced. Therefore, they have more influence on neuronal activity at voltages below the action potential threshold. Panel E also shows a slight difference between the *MmErg3* channel and the *NvErg1* channel – the *NvErg1* channel inactivates faster than the *MmErg3* channel. However, it was observed while *hERG1* was being characterized for another experiment in lab that the inactivation rate is very similar to *NvErg1*, and thus *NvErg1* is not an outlier of the *Erg* subfamily channels in higher mammals. Inactivation could indicate several different physiological roles, and as previously discussed a likely function of inactivation is to regulate plateau action potentials similarly to the *hERG1* channel (Grunnet et al., 2008).

Panel F shows the activation rate of the *NvErg1* channel. As previously mentioned, the *NvErg1* channel has activation as well as inactivation; therefore, measuring the activation rate directly from the depolarization steps would not have been accurate. Instead, we used a tail envelope protocol. In this protocol the oocytes rested at -100mV and then were depolarized to +40mV for pulses that ranged in time from 5ms to 500ms. Then, the voltage was brought back

down to -120mV. This protocol was arranged to discern the activation rate without the inactivation hindering computation. The repolarization to -120mV gives any channel that has been inactivated the chance to recover and pass current before closing because the recovery of the channel is fast and the deactivation is slow; therefore, we could measure how many channels opened in the previous pulse. Note that in this panel, because the sweeps were done at very low voltage, the current is an inward potassium current which is to be expected below the E_K^+ (-90mV) in our recording solution. Each pulse gave a peak downwards and the peaks increased in amplitude with increasing depolarization pulse time. This data was put into a peak current plot which shows an approximation of the activation rate and can be seen in Panel G. One can see that the rate curve for *NvErg1* is virtually identical to that of *MmErg3*, highlighting the similar gating kinetics seen in both channels.

The data in Figure 5 show that the gating phenotype of *NvErg1* is similar to that of the mammalian *Erg* channels such as *MmErg3*. The traces seen in Panels A and B have the same characteristic shape which is influenced by similar voltage dependence, inactivation rates, and activation rates seen in both *NvErg1* and *MmErg3*. However, the *NvErg1* channel is dissimilar to *DmErg*. Recently, Fregestad et al. (2010) used the gene *Dao*, a regulator of the *DmErg* channel, to functionally express *DmErg*, previously uncharacterized. In this article they show a trace recording, and the channel is very similar to *DmEag*, which does not have inactivation like the *MmErg3* or *NvErg1* channel. It is interesting that the *DmErg* channel both lacks the PAS domain and differs from both the old Cnidarian characteristics and evolutionarily newer mammalian characteristic. Therefore, our data suggests that the function of *Erg* channels in plateau action potentials may be ancient, and this function may have been lost in flies.

As outlined in our experimental aims, the next step in analyzing the *NvErg1* channel was to examine its pH sensitivity. Figure 6 is a schematic of the EAG family channels which shows the location of family-specific acidic residues. These residues are located in the external voltage

sensor (red) in addition to an acidic residue found in other voltage-gated potassium channels (green) and confer high sensitivity of voltage-dependent gating to external pH changes in *Eag*, *Erg* and *Elk* channels. Previous work done in the lab indicated that the conserved S3 aspartate is involved in pH sensitivity (Kazmierczak et al., submitted). Interestingly, the *NvErg1* and *NvEag1* channels do not have this residue and instead the *NvErg1* channel has a glutamate residue and the *NvEag1* channel has a glycine residue. Therefore, to study pH sensitivity, we mutated the residues found in *Nematostella* to the residue conserved in higher mammalian EAG family channels.

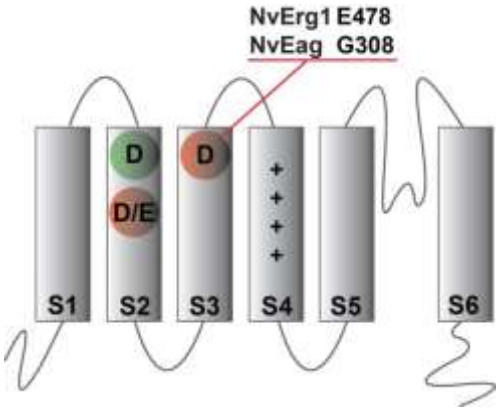

Figure 6. Ether-a-go-go family-specific acidic residues in the voltage sensor (Kazmierczak et al., submitted)

Figure 7 shows the pH sensitivity of the *NvErg1* channel, the mutated *NvErg1E478D* and the mouse *MmErg3* channels. Example traces are shown at pH 8, which is always shown in red, pH 7, which is always shown in black, and pH 6, which is always shown in blue. Qualitatively, one can see that the change in current conductance due to external pH is very large in the wild type *NvErg1* channel which possesses the glutamate residue, based on the amplitude of the traces at each pH. Additionally, the voltage dependence is also pH sensitive, which can be seen by looking at the way the shape of the example traces change with pH. The E478D mutation to the mammalian EAG-specific residue aspartic acid greatly reduces the effect of pH on voltage-dependent activation but does not eliminate much of the independent current conductance

dependence on pH. The *MmErg3* channel, which possesses the aspartic acid residue, in contrast to the *NvErg1* wild type channel, has much less pH-dependent conductance change. However, *MmErg3* does have some voltage activation pH dependence. It is possible that the increased current conductance pH dependence seen in the *NvErg1* channel is due to glutamate's larger size and thus increased efficiency in titrating protons.

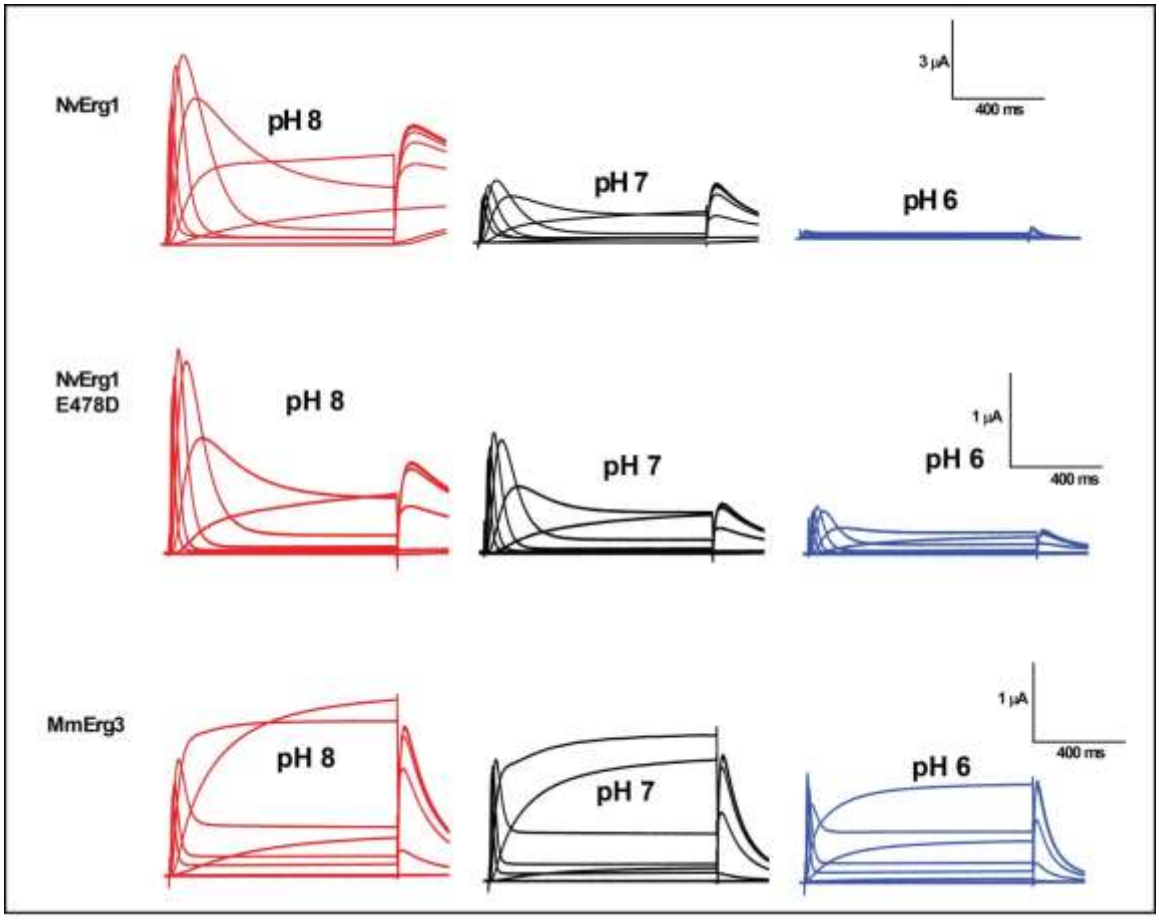

Figure 7. *NvErg1*, *MmErg3* and *NvErg1 E478D* currents recorded in bath solutions of pH 8, 7, 6

Figure 8 shows the G/V curves for *NvErg1*, *NvErg1E478D*, and *MmErg3* at pH 8 (red), pH 7 (black), and pH 6 (blue). The G/V curves here were taken from isochronal tail currents taken at -70mV with n = 6-15. This figure illustrates the effect of pH on voltage dependence of activation and the extent to which it is eliminated in the *NvErg1E478D* mutant. One can see that in the G/V curves of the *NvErg1* expression at different pH values are visually separated with the

pH 8 being most hyperpolarized and pH 6 being the most depolarized as predicted by previous research. The *MmErg3* curves at the different pH values are also separated, and one can see that the difference between G/V curves at different pH in *MmErg3* appears to be greater than in the mutant *NvErg1E478D*.

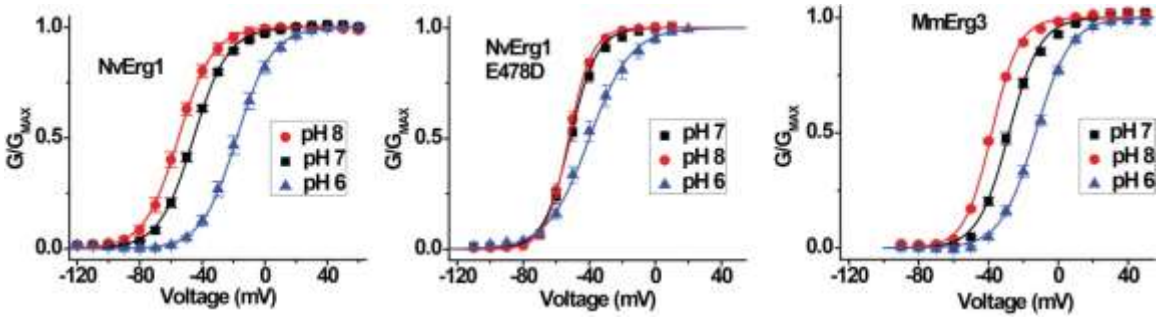

Figure 8. Voltage activation curves for *NvErg1, NvErg1 E478D* and *MmErg3* in external solutions of pH 8, pH 7 and pH 6

Table 1 shows the V_{50} values that quantify the differences seen in Figure 8.

	NvErg1	NvErg1E478D	MmErg3
pH 8	-55.3 ± 1*	-52.4 ±1	-38.2 ± 0.4*
pH 7	-45.6 ± 0.8*	-51.6 ± 1	-28.3 ± 1
pH 6	-18 ± 2*	-40± 3*	-13 ± 3*

Table 1. V_{50} values from G/V curves of *NvErg1*, *NvErg1E478D*, and *MmErg3*.

The V_{50} values quantitatively show the influence of pH on voltage dependent activation in each of the channels. The asterisks indicate V_{50} values that are significantly different than those at pH 7 and indicate a p-value less than 0.01. This is greater than standard field requirement (p=0.05), however, the p-value of V_{50} difference between pH 8 and pH 7 for *NvErg1E478D* outside of this range as well, thus was not statistically significant. The *NvErg1* and *MmErg3* V_{50} values at pH 8 and 6 were significantly different than the V_{50} value at pH 7. The *NvErg1* channel had a 37.2 ± 2 mV depolarized shift from pH 8 to pH 6. In contrast, the *NvErg1E478D* mutant had a depolarized shift of only 12.3 ± 3 mV from pH 8 to pH 6 which was less than the shift in *MmErg3* of 25.2 ± 1 mV. The difference in shift between the wild type *NvErg1* and mutant *NvErg1E478D* mutant was statistically significant with $p < 0.0001$. This clearly demonstrates

how much of the pH sensitivity of the *NvErg1* channel was dependent on the glutamate residue that was originally present in the channel. Therefore, in *Erg* channels, the mammalian phenotype is seen in *Nematostella* and implies that pH sensitivity has been conserved since Cnidarians. The specific type of pH sensitivity differs between the two channels, but *MmErg3* and *NvErg1* are both sensitive to external pH.

The *NvEag1* channel was also functionally characterized, and the results can be seen in Figure 9. The example traces were recorded using the same step protocol used for Figure 5, but was modified so that the tails were recorded at -40 mV. The traces were taken in one second sweeps when I recorded the *NvEag1* channel current as well as the *NvErg1* channel current, which explains why it appears shorter than the *MmEag2* trace which used the same step protocol but prolonged it for two seconds. Panel A and B show the similarity between the shape of the *NvEag1* and *MmEag2* channels, including a fast activation and equally fast deactivation. This is a typical *Eag* subfamily characteristic that has been conserved. *Eag* subfamily channels differ from *Erg* subfamily channels in that there is no inactivation during sustained depolarization. Panel C shows the G/V curves of both *NvEag1* and *MmEag2* taken from n=6-11, and one can see that the shape is similar; however, there are a few differences. First, the *NvEag1* channel is depolarized compared to *MmEag2* and appears to be more voltage dependent based on the steepness of the curve. The V_{50} value of the *NvEag1* channel at pH 7 is -26.4 ± 1 and the V_{50} value of the *MmEag2* channel at pH 7 is -71 ± 3 mV which can be seen in Table 2 (Kazmierczak et al., submitted).

There is a large difference in voltage activation between *NvEag1* and *MmEag2*, however the current kinetics of the two channels as seen with the example traces are very similar. Other *Eag* channels have more similar voltage ranges to *NvEag1*. Rat *Eag* has a very similar voltage of activation as the *NvEag1* channel, the G/V curve looks very similar, and it opens around -40mV,

which is more similar to *NvEag1* which opens around -80 mV (Terlau et al., 1996). Despite the difference in voltage activation, the characteristics of the *NvEag1* channel are very similar to those of *MmEag2* and additionally, the channel is still active at some sub-threshold voltages, therefore confirming the conserved function.

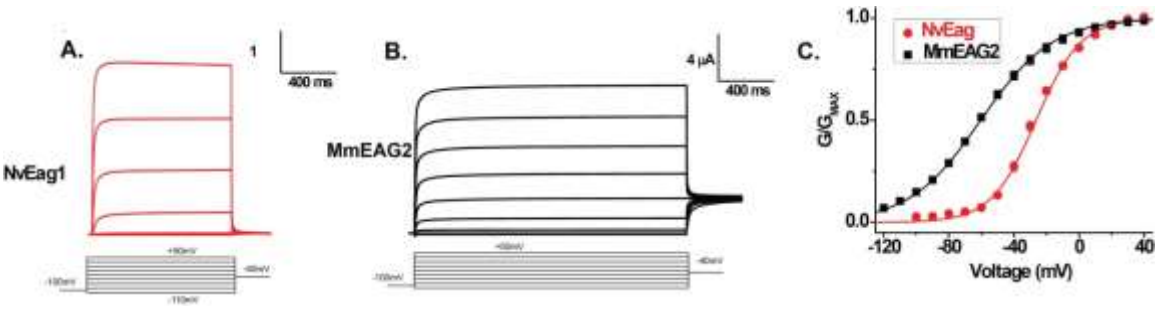

Figure 9. Functional expression of *NvEag* and comparison to *MmEag2*.

Figure 10 was created from data points from traces of *NvEag1* and *NvEag1G308D* at pH 8, 7, and 6 with n=6-8.

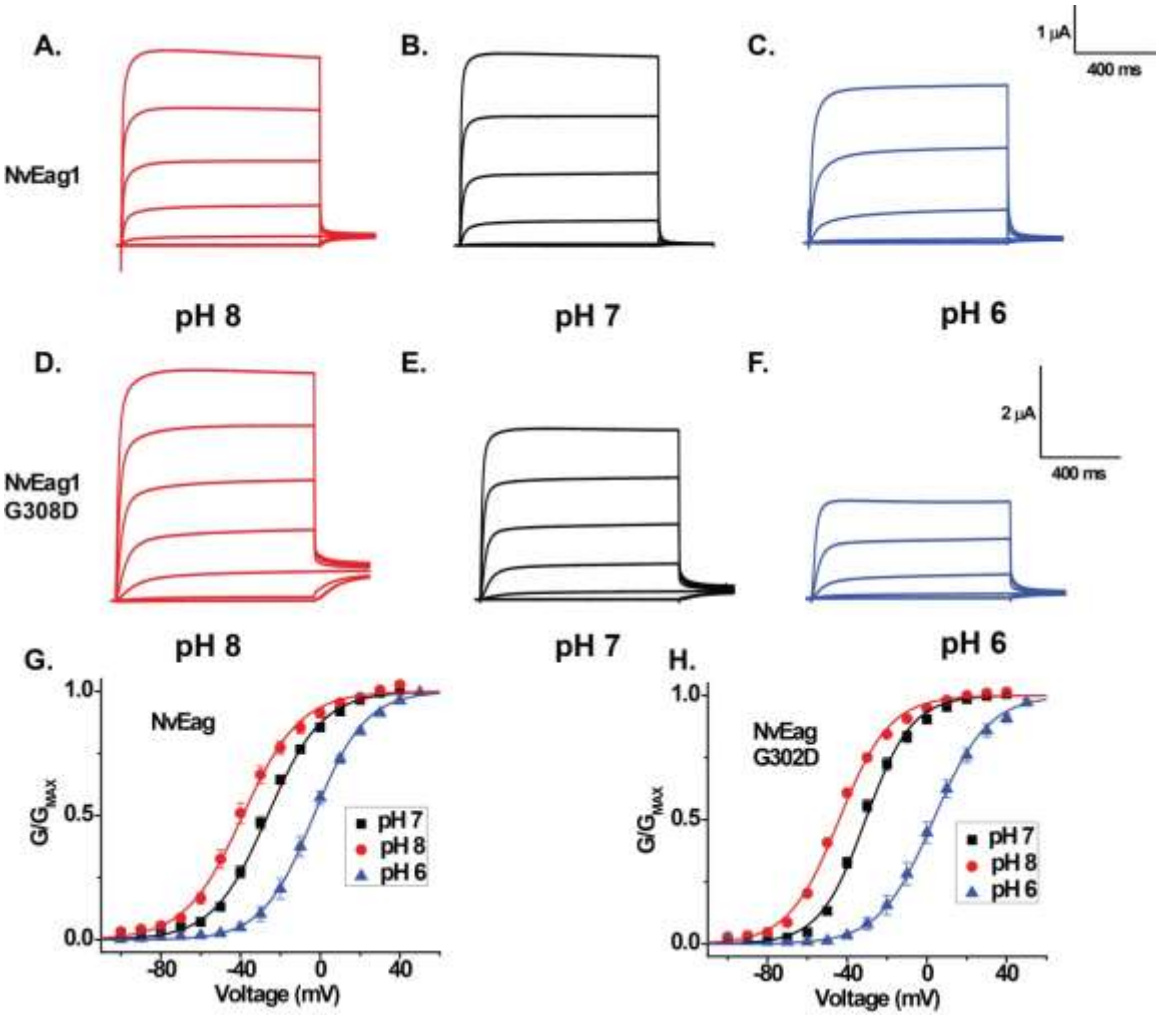

Figure 10. Voltage-activation of *NvEag1* is highly sensitive to external pH.

One can see that unlike *NvErg1* there is not a large change in conductance due to pH in the wild type *NvEag1* channel. However, there is a significant change in voltage dependence due to pH as can be seen by panel G which compares the G/V curves for *NvEag1* at the different pH solutions. As with the *NvErg1* curves, pH 8 is hyperpolarized relative to pH 7 and pH 6 is relatively depolarized. The mutant, *NvErg1G380D*, has a greater conductance change due to pH as well as a greater change in voltage dependent pH sensitivity. This is expected, as the nonpolar

glycine residue changed to the negatively charged glutamate was predicted to confer more pH sensitivity upon the channel. Table 2 contains the V_{50} values that quantify these curves.

	NvEag1	NvEag1G308D	MmEag2
pH 8	-39 ± 2*	-44.1 ± 0.7*	-95 ± 3*
pH 7	-26.4 ± 1	-30.8 ± 1	-71 ± 3
pH 6	-3.2 ± 1*	3.3 ± 3*	-24 ± 2*

Table 2. V_{50} values from *NvEag1, NvEag1G380D, MmEag2* (Kazmierczak et al., submitted)

From this table, one can see that the *NvEag1* channel is sensitive already without the acidic EAG-family specific charge, yet the *NvEag1G380D* mutant is even more pH sensitive. From pH 6 to pH 8 there is a 35.71 ± 3 mV shift in the *NvEag1* channel; in the *NvEag1G380D* mutant there is a 47.33 ± 3 mV shift from pH 6 to pH 8. There is a statistically significant difference between the shift in the mutant *NvEag1G380D* and the wild type *NvEag1* channel with $p< 0.05$. The *MmEag2* channel is even more pH sensitive and shifts 71 mV between pH 8 and pH 6. Once again, the asterisks indicate that all channels had pH 8 and pH 6 V_{50} values that were significantly different than the pH 7 V_{50} values and had $p<0.01$. From this and the *NvErg1* channel data, one can conclude that pH sensitivity has indeed been a conserved property of *Erg* and *Eag* subfamily channels.

We found throughout this project that the EAG family channels we studied were similar to their mammalian counterparts in all three aspects that we studied: gating kinetics, sub-threshold activation, and pH sensitivity. The gating kinetics were almost identical in the *Nematostella* channels and the mouse channels with which we compared them. The *NvErg1* channel has the characteristic *Erg* subfamily inactivation (in mammals, as discussed this is not present in DmErg). Additionally, the *NvEag1* channel has the rapid activation and deactivation that is seen in higher animals. The sub-threshold activation has been conserved throughout the history of EAG channels since Cnidarians, as seen in both *NvErg1* and *NvEag1*. pH sensitivity was also found to in both *Nematostella* EAG family channels, although they responded

differently to the mutagenesis to the EAG-family specific residue. The *NvEag1* channel was significantly more pH sensitive with the EAG-family specific aspartate as opposed to nonpolar glycine, whereas the *NvErg1* channel was significantly less pH sensitive with the aspartate compared to its native glutamate, hypothesized to confer greater sensitivity due to size. Therefore, EAG family channel gating kinetics, sub-threshold activation and pH sensitivity appear to be fundamental properties of the channels and significant for physiological function.

In future studies we hope to elucidate the entire functional evolution of EAG family channels. This will be accomplished by successful cloning and expression of *NvElk1*, as well as *NvErg4* which was cloned but not functionally expressed during this thesis project. We hypothesize this channel may behave more similarly to *DmErg*, due to its lack of a PAS domain. Additionally, expression patterns will be determined and compared with behavioral experiment results utilizing transgenic techniques. We want to disrupt the function of the *NvErg1* channel and predict it may disrupt wave contractions similar to cardiac contractions in humans that are disrupted by mutations to the *hERG1* channel (Sanguinetti and Tristani-Firouzi, 2006). It is possible that *Nematostella* require plateau action potentials to function.

The relationship between the EAG family channel ancestor and modern day EAG family channels will hopefully be discovered using the Ctenophore genome and cloning and functional expression of an EAG-like channel. The Ctenophore genome contains one EAG-like gene which is an outgroup to the three subfamilies of EAG family genes seen in higher animals due to its ancestral nature (Schnitzler et al., 2013). Therefore, we would like to use Ctenaphores to determine which functional properties evolved first, even before Cnidarian functional characteristics. In short, there is a plethora of future work that was sparked by the discoveries of this thesis, and this work will increase knowledge of the fundamental functions of EAG family channels and thus, their physiological role.

REFERENCES

Altschul SF, Madden TL, Schaffer AA, Zhang J, Zhang Z, Miller, W., Lipman, D.J. 1997. Gapped BLAST and PSI-BLAST: a new generation of protein database search programs. *Nucleic Acids Res* 25: 3389–3402.

Anumonwo, J.M., J. Horta, M. Delmar, S.M. Taffet, and J. Jalife. 1999. Proton and zinc effects on HERG currents. *Biophysical journal*. 77:282-298.

Berube, J., M. Chahine, and P. Daleau. 1999. Modulation of HERG potassium channel properties by external pH. *Pflugers Archiv : European journal of physiology*. 438:419-422.
Proc Natl Acad Sci U S A. 2010 March 23; 107(12): 5617–5621.

Fergestad, T., Sale, H., Bostwick B., Schaffer, A., Ho, L., Robertson, G.A., Ganetzky, B. 2010. A *Drosophila* behavioral mutant, *down and out* (*dao*), is defective in an essential regulator of Erg potassium channels. *Proc Natl Acad Sci USA*. 107(12):5617-21

Hardman, R.M., and I.D. Forsythe. 2009. Ether-a-go-go-related gene K+ channels contribute to threshold excitability of mouse auditory brainstem neurons. *J Physiol*. 587:2487-2497.

Hille, Bertil. *Ion Channels of Excitable Membranes*. 3rd ed. Sunderland: Sinauer Associates, Inc., 2001. 131-167. Print.

Jegla, T.J., Zmasek, C.M., Baralov, S., Nayak, S.K. 2009. Evolution of the Human Ion Channel Set. *Combinatorial Chemistry & High Throughput Screening*. 12:2-23

Jegla T, Marlow HQ, Chen B, Simmons DK, Jacobo SM, et al. (2012) Expanded Functional Diversity of Shaker K^+ Channels in Cnidarians Is Driven by Gene Expansion. *PLoS ONE* 7(12): e51366. doi:10.1371/journal.pone.0051366

Jo, S.H., J.B. Youm, I. Kim, C.O. Lee, Y.E. Earm, and W.K. Ho. 1999. Blockade of HERG channels expressed in Xenopus oocytes by external H+. *Pflugers Archiv : European journal of physiology*. 438:23-29.

Marlow, H.Q., Srivastava. M., Matus, D.Q., Rokhsar, D., Martindale, M.Q. 2009. Anatomy and Development of the Nervous System of Nematostella vectensis, an Anthozoan Cnidarian. *Developmental Neurobiology*.69(4):235-54.

Microsoft. Microsoft Excel. Redmond, Washington: Microsoft, 2003. Computer Software

Putnam, N.H., Srivastava, M., Hellsten, U., Dirks, B., Chapman, J., Salamov, A., Terry, A., Shapiro, H., Lindquist, E., Kapitonov, V.V., Jurka, J., Genikhovich, G., Grigoriev, I.V., Lucas, S.M., Steele, R.E., Finnerty, J.R., Technau, U., Martindale, M.Q., Rokhsar, D. 2007. Sea Anemone Genome Reveals Ancestral Eumetazoan Gene Repertoire and Genomic Organization. *Science.* 317:86-94.

Renfer, E., Amon-Hassenzahl A., Steinmetz, P.R., Technau U., 2010. A muscle-specific transgenic reporter line of the sea anemone, Nematostella vectensis. *Proc Natl Acad Sci USA.* 107(1):104-8

Ronquist F, Huelsenbeck JP 2003. MrBayes 3: Bayesian phylogenetic inference under mixed models. Bioinformatics 19: 1572–1574.

Shi, W., H.S. Wang, Z. Pan, R.S. Wymore, I.S. Cohen, D. McKinnon, and J.E. Dixon. 1998. Cloning of a mammalian elk potassium channel gene and EAG mRNA distribution in rat sympathetic ganglia. *J Physiol*. 511 (Pt 3):675-682.

Schnitzler, C.E., Pang, K., Powers, M.L., Reitzel, A.M., Ryan, J.F., Simmons, D., Tada, T., Park, M., Gupta, J., Brooks, S.Y., Blakesley, R.W., Yokoyama, S., Haddock, S.H.D., Martindale, M.Q., Baxevanis, A.D. 2012. Genomic organization, evolution, and expression of photoprotein and opsin genes in Mnemiopsis leidyi: a new view of ctenophore photocytes. *BMC Biology* 10:107

Srivastava M, Begovic E, Chapman J, Putnam NH, Hellsten U, et al. 2008. The Trichoplax genome and the nature of placozoans. *Nature* 454: 955–960.

Tamura K, Peterson D, Peterson N, Stecher G, Nei M, et al. 2011. MEGA5: molecular evolutionary genetics analysis using maximum likelihood, evolutionary distance, and maximum parsimony methods. Mol Biol Evol 28: 2731–2739.

Terai, T., T. Furukawa, Y. Katayama, and M. Hiraoka. 2000. Effects of external acidosis on HERG current expressed in Xenopus oocytes. *Journal of molecular and cellular cardiology*. 32:11-21.

Terlau, H., J. Ludwig, R. Steffan, O. Pongs, W. Stuhmer, and S.H. Heinemann. 1996. Extracellular Mg2+ regulates activation of rat eag potassium channel. *Pflugers Archiv : European journal of physiology*. 432:301-312.

Wickenden, A. 2002. K^+ channels as therapeutic drug targets. *Pharmacology and Therapeutics*. 94:157-182.

Zhang, X., F. Bertaso, J.W. Yoo, K. Baumgartel, S.M. Clancy, V. Lee, C. Cienfuegos, C. Wilmot, J. Avis, T. Hunyh, C. Daguia, C. Schmedt, J. Noebels, and T. Jegla. 2010. Deletion of the potassium channel Kv12.2 causes hippocampal hyperexcitability and epilepsy. *Nature neuroscience*.
13:1056-1058.

ACADEMIC VITA

Alexandra Martinson

Ali.martinson308@gmail.com

Education

B.S., Biology, Neuroscience Option, Honors in Biology, Minor in Spanish, 2013, Pennsylvania

State University, State College, Pennsylvania

Work Experience

*Dr. Jegla's Lab, University Park, PA, Research Assistant***,** January 2011-present

- Created multiple vectors in DNA cloning project
- Determined ion channel properties through electrophysiology
- Completed thesis project research to be published in near future

Dr. Makova's Lab, University Park, PA, Research Assistant, January 2010-December 2010

- Collaborated to sequence equine DNA
- Sequenced mitochondrial DNA from two individuals

Hunterdon Medical Center, Volunteer, May 2010-August 2010

- Transported patients to and from various hospital locations
- Assisted nurses and attended to patient needs

Leadership

Schreyer Honors College, Freshmen Orientation Lead Mentor, January 2012-September 2012

- Planned and orchestrated a 3 day orientation for 300 incoming scholars
- Led 14 team leaders as well as 89 mentors
- Interacted with staff, mentors and community members to execute 23 separate events

Science Lionpride

- THON Family Relations Chair, May 2012- present
- Secretary and Treasurer , Fall 2011- Spring 2012
- Relay for Life Chair**,** Spring 2011

Activities

THON Hospitality Committee, September 2011-February 2013

NSSHLA, Fall 2011 – Fall 2012

Professional Presentations

Society for Neuroscience Conference, October 2012

- Presented poster containing thesis research

Pennsylvania State University Undergraduate Poster Session, April 2012

- Presented thesis research completed during the Spring 2012 semester

Awards

Undergraduate Research Grant, Pennsylvania State University,Spring 2010 and Spring 2012

Biology Department Scholarship, Pennsylvania State University, Spring 2012

Scholarship for Academic Excellence, Schreyer Honors College, Fall 2009- present

President's Freshmen Award, Pennsylvania State University, Spring 2010